

## Redox Reactions of a Dinuclear Manganese Complex – the Influence of Water

Philipp Kurz,<sup>[a][‡]</sup> Magnus F. Anderlund,<sup>[a]</sup> Nizamuddin Shaikh,<sup>[a][‡‡]</sup> Stenbjörn Styring,<sup>[a]</sup> and Ping Huang\*<sup>[a]</sup>**Keywords:** Manganese / N,O ligands / Biomimetic synthesis / Redox chemistry / EPR spectroscopy

The redox properties of the dinuclear manganese complex  $[\text{Mn}^{\text{III,III}}_2\text{L}(\mu\text{-OAc})_2]^+$  (**1**) (where L is the trianion of the heptadentate ligand 2,6-bis[(3,5-di-*tert*-butyl-2-hydroxybenzyl)-(2-pyridylmethyl)amino]methyl-4-methylphenol) were studied in acetonitrile solutions containing different concentrations of water. Electrochemical reactions as well as reactions with different chemical and photochemical redox reagents were monitored, using a variety of analytical techniques, namely cyclic voltammetry, UV/Vis spectroelectrochemistry, and EPR spectroscopy. We found that even small concentrations of water influence the compound's redox behaviour significantly, especially the oxidation reactions. As a consequence, the presence of water reduces the overall potential span needed to reach the highest oxidation state observed

for **1** ( $\text{Mn}^{\text{III,IV}}_2$ ) from its most reduced state ( $\text{Mn}^{\text{II,II}}_2$ ) to about 1.1 V. Higher oxidation states of **1** are stabilized, most likely by water coordination and the formation of  $\mu$ -oxido bridge(s) between the two manganese atoms. For reducing conditions, an unprecedented 25-line EPR signal was observed, which might originate from reduced **1** in its  $\text{Mn}^{\text{II,II}}_2$  or  $\text{Mn}^{\text{II,III}}_2$  state after considerable ligand rearrangement. As complexes like **1** have been designed to act as potential water oxidation catalysts, the complicated redox- and ligand-exchange chemistry found for **1** in the presence of water, its intended substrate, might be exemplary for many of the dinuclear manganese compounds currently under investigation.

(© Wiley-VCH Verlag GmbH & Co. KGaA, 69451 Weinheim, Germany, 2008)

## Introduction

The research interest in multinuclear manganese compounds originates to a large extent from two long-term, bio-inspired goals: firstly, it is necessary to design and study model compounds to achieve a detailed understanding of the manganese-containing oxygen-evolving complex (OEC), the site of water oxidation in natural photosynthesis;<sup>[1–5]</sup> secondly, a better understanding of manganese redox chemistry should assist in the design of artificial, bio-mimetic water-oxidation catalysts to be used for solar energy conversion.<sup>[6–11]</sup>

In the natural OEC, the catalytic  $\text{CaMn}_4$  cluster cycles through five oxidation states to accumulate enough oxidation power to catalyze the water-oxidation reaction ( $2\text{H}_2\text{O} \rightarrow \text{O}_2 + 4\text{H}^+ + 4\text{e}^-$ ). The complete catalytic cycle operates within a remarkable narrow potential range of 0.3 V.<sup>[12–14]</sup> Even though the detailed mechanism remains unclear, the deprotonation of water molecules coordinated to the  $\text{CaMn}_4$  cluster during the catalytic cycle seems essen-

tial to achieve such a compressed range for the cluster's redox reactions.<sup>[2,14,15]</sup>

Numerous synthetic manganese complexes have been designed to mimic key features of the OEC. For this purpose, they should at least contain two manganese centers to accommodate the necessary oxidation states and show multi-step redox stability. Above all, the ability to bind water, the substrate molecule, is of most concern. The mechanism proposed for the OEC suggests that water binding and O–O bond formation take place when the enzyme advances towards higher manganese oxidation states. Therefore, it is our main interest to investigate how redox properties of the synthetic manganese complexes intended to be OEC mimics are affected in the presence of water.

A prominent class among these compounds are assemblies where two manganese ions are bridged by  $\mu$ -alkoxy oxygen atoms part of heptadentate ligand frameworks.<sup>[9]</sup> Thus, four coordination sites of each manganese center are occupied by chelating ligands. As the usual coordination number for manganese is 6, with 5 or 7 found less frequently as well,<sup>[16–20]</sup> one to three possible water-binding sites per manganese centre are available.

The coordination sphere of the  $\text{CaMn}_4$  cluster of Photosystem II is dominated by carboxylato ligands and histidine groups provided by the protein scaffold.<sup>[21,22]</sup> These features are incorporated in a series of our synthetic dinuclear manganese complexes, where we have used bridging acetato groups together with pyridine rings as ligands for the manganese centers.<sup>[23]</sup>

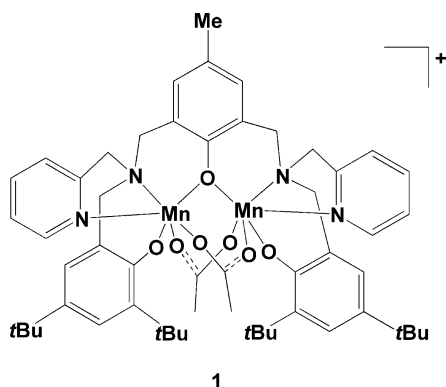
[a] Department of Photochemistry and Molecular Science Ångström Laboratory, Uppsala University, Box 523, 75120 Uppsala, Sweden  
E-mail: ping.huang@fotomol.uu.se

[‡] Current address: Institut für Anorganische Chemie, Christian-Albrechts-Universität zu Kiel, Otto-Hahn-Platz 6/7, 24098 Kiel, Germany

[‡‡] Current address: Institute for Materials Chemistry and Engineering, Kyushu University, 6-1 Kasuga Koen, Kasuga, Fukuoka 8168580, Japan

Supporting information for this article is available on the WWW under <http://www.eurjic.org> or from the author.

We present here the detailed study of the redox behavior of a dimeric manganese compound,  $[\text{Mn}^{\text{III,III}}_2\text{L}(\mu\text{-OAc})_2]^+$  (**1**) in the presence of water (where L is the trianion of 2,6-bis{[(3,5-di-*tert*-butyl-2-hydroxybenzyl)(2-pyridylmethyl)-amino]methyl}-4-methylphenol; Scheme 1). In this complex, each of the two manganese atoms is coordinated by a pyridine ring, a phenolato group and a tertiary amino function of the heptadentate ligand. Additionally, the metal centers are bridged by a central phenolato and two bidentate acetato ligands. These acetato ligands are expected to be accessible for substitution by aquo ligands in a manner similar to that shown in previous studies of related complexes.<sup>[24,25]</sup> As compounds like **1** have been designed to act as water-oxidation catalysts, the influence of  $\text{H}_2\text{O}$  on the redox processes of **1** was the focus of this study.



Scheme 1.

So far, the reactivity of **1** has been investigated in organic solvents, mostly acetonitrile (MeCN).<sup>[26]</sup> In this work, we examined the redox properties of **1** in MeCN solutions in the presence of  $\text{H}_2\text{O}$  in order to gain new insights into the water influence on the redox properties of **1**.

## Results and Discussion

### Mass Spectrometry

Mass spectra were recorded for solutions of **1** in dry acetonitrile as well as MeCN containing 0.5 M  $\text{H}_2\text{O}$  (see Supporting Information, Figure S1). In both cases, the parent peak of cation **1**<sup>+</sup> is the species dominating the mass spectrum with only very little fragmentation observed. In dry solution, single acetate loss resulting in a mass corresponding to  $[\text{1} - \text{AcO}]^+$  is detected for about 5% of **1**. For a solution containing 0.5 M  $\text{H}_2\text{O}$ , a fraction of less than 5% of **1** exchanges acetato ligands for water at room temperature within 30 min, indicating that no significant acetato ligand loss occurs for the  $\text{Mn}^{\text{III,III}}_2$  compound at this water concentration.

### Electrochemistry

Cyclic voltammograms of complex **1**, in the absence and presence of water, are shown in Figure 1. As reported earlier,<sup>[26]</sup> complex **1** is oxidized irreversibly in dry MeCN at

potentials above +0.60 V, with a potential at the half height of the oxidation wave of +0.73 V (Figure 1, Table 1). In the presence of water, the oxidation becomes slightly more facile as the peaks shift towards lower potentials. In the presence of 0.5 M  $\text{H}_2\text{O}$ , an oxidation potential reduced by nearly 40 mV is observed. Additionally, a small back-wave is found when the water concentration is increased to 5 M (Figure 1a), indicating that at least a fraction of the compound can be re-reduced after oxidation in the presence of water in contrast to reactions under dry conditions. However, the reduction occurs at a potential 0.2 V lower than the oxidation peak, indicating the involvement of a chemical modification in addition to the one-electron redox event.

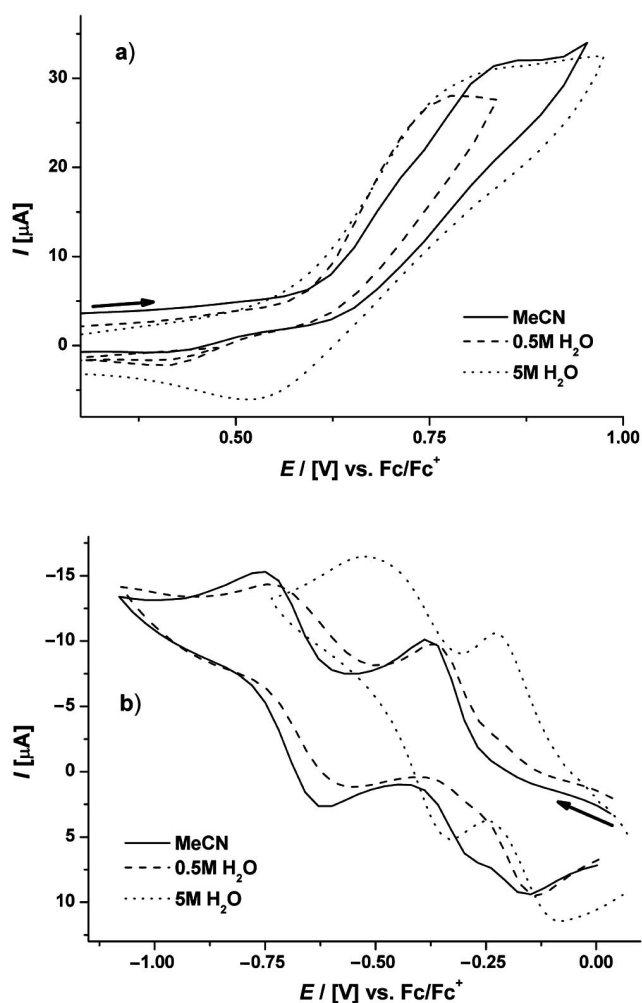


Figure 1. Cyclic voltammograms ( $0.1 \text{ V s}^{-1}$ ) of the oxidation (top) and reduction (bottom) of **1** in MeCN (1 mM **1**, 0.1 M TBA·ClO<sub>4</sub>) at room temperature containing increasing concentrations of water.

Table 1. Electrochemical data.

Redox process	$E_{1/2}$ [V] ( $\Delta E_p$ [mV])		
	MeCN	0.5 M $\text{H}_2\text{O}$	5 M $\text{H}_2\text{O}$
$\text{Mn}^{\text{III,IV}}_2/\text{Mn}^{\text{III,III}}_2$	0.73 <sup>[a,b]</sup>	0.69 <sup>[a]</sup>	0.69 <sup>[a]</sup>
$\text{Mn}^{\text{III,III}}_2/\text{Mn}^{\text{II,III}}_2$	−0.35 (100) <sup>[b]</sup>	−0.24 (230)	−0.15 (150)
$\text{Mn}^{\text{II,III}}_2/\text{Mn}^{\text{II,II}}_2$	−0.69 (140) <sup>[b]</sup>	−0.65 (180)	−0.43 (190)

[a] Irreversible oxidation. [b] See also ref.<sup>[26]</sup>

At reducing potentials, two reversible waves, assigned to the  $\text{Mn}^{\text{III,III}}_2/\text{Mn}^{\text{II,III}}_2$  ( $E_{1/2} = -0.35$  V) and the  $\text{Mn}^{\text{II,III}}_2/\text{Mn}^{\text{II,II}}_2$  ( $E_{1/2} = -0.69$  V) redox couples are observed in dry MeCN.<sup>[26]</sup> Both processes show large peak splits (100 and 140 mV, respectively; Figure 1b). For the  $\text{Mn}^{\text{III,III}}_2/\text{Mn}^{\text{II,III}}_2$  redox couple, the re-oxidation signal seems to consist of at least two peaks, positioned at  $-0.29$  and  $-0.15$  V. This has been attributed to ligand rearrangement processes.<sup>[26]</sup> In the presence of water, both reduction potentials shift to significantly higher potentials, and the re-oxidation at  $-0.29$  V is not found any longer (Figure 1b, Table 1). For a water concentration of 5 M, the first reduction is shifted by as much as +200 mV, the second by +260 mV.

We thus find a pronounced effect of water on the redox potentials of **1**. Overall, the presence of water enhances the redox reversibility slightly and compresses the separation in the potentials between the reduction to the  $\text{Mn}^{\text{II,II}}_2$  state and the onset of oxidation of the  $\text{Mn}^{\text{III,III}}_2$  state by over 300 mV to about 1.1 V. In order to obtain a better insight into the electrochemical redox products in the presence of water, bulk electrolyses were carried out at selected potentials, and solutions were further examined using different spectroscopic techniques after electrolysis as described below.

### UV/Vis Spectroelectrochemistry

When dissolved in MeCN containing 0.5 M  $\text{H}_2\text{O}$ , **1** forms a dark red solution with strong UV absorption bands below 350 nm. In the visible region, an absorption peak at 410 nm is observed with a shoulder at wavelengths above 500 nm (Figure 2). After one-electron reduction to the  $\text{Mn}^{\text{II,III}}_2$  state, these bands become considerably weaker and shift to slightly lower wavelengths with a peak at 400 nm. Further reduction results in a nearly colourless solution with weak, unstructured absorption detected above 350 nm. It is known that structurally related complexes are usually

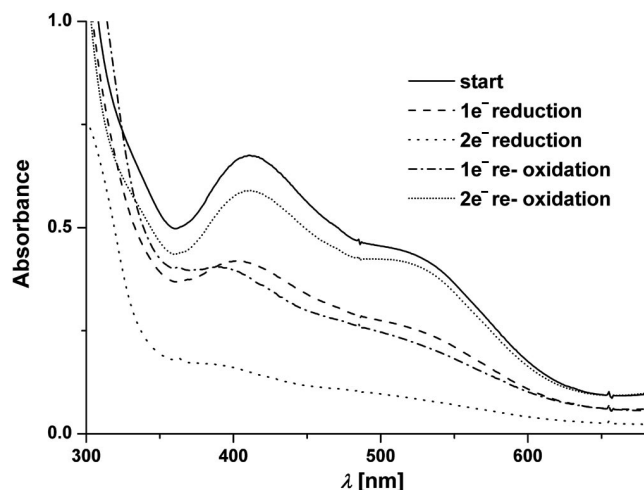


Figure 2. Absorption spectrum of **1** (1 mM in MeCN/0.5 M  $\text{H}_2\text{O}$ , —) in an OTTE cell. Spectra recorded after stepwise reduction at  $-0.51$  V (---),  $-1.01$  V ( $\cdots$ ), and subsequent re-oxidation at  $-0.51$  V (— · —) and  $+0.14$  V (— · —).

colourless in their  $\text{Mn}^{\text{II,II}}_2$  redox states.<sup>[26–28]</sup> The gradual colour loss under reducing conditions is in agreement with the conversion of  $\text{Mn}^{\text{III}}$  to  $\text{Mn}^{\text{II}}$  in **1**.

The intermediate spectrum after one-electron re-oxidation shows only small changes compared to the  $\text{Mn}^{\text{II,III}}_2$  spectrum and the original absorption spectrum is obtained again upon re-oxidation. It is, however, reduced in intensity, indicating that about 10% of the colourless species formed after two-electron reduction is not re-oxidized, while most of the molecules cycle reversibly between the  $\text{Mn}^{\text{III,III}}_2$  and  $\text{Mn}^{\text{II,II}}_2$  states.

### EPR Spectroscopy

#### Electrochemical Redox Reactions

It has been established that the two  $\text{Mn}^{\text{III}}$  ions in **1** are weakly antiferromagnetically coupled, and **1** is thus expected to be EPR-silent.<sup>[26]</sup> Indeed, no EPR signals, neither in perpendicular nor parallel mode, were found for 1 mM solutions of **1** in MeCN.<sup>[29]</sup>

If **1** is oxidized electrochemically in the presence of 0.5 M  $\text{H}_2\text{O}$  at an applied potential of  $+0.64$  V, the solution after electrolysis gives rise to a characteristic  $\text{Mn}^{\text{III,IV}}_2$  16-line EPR spectrum (Figure 3b). The multiline signal is about 1110 G wide and centred at  $g \approx 2$  with lines split between 65 and 70 G. Such spectral features have been reported for a mono( $\mu$ -oxido)-bridged  $\text{Mn}^{\text{III,IV}}_2$  core and in good agreement with other mono( $\mu$ -oxido)-bridged  $\text{Mn}^{\text{III,IV}}_2$  complexes.<sup>[30–32]</sup> The mono( $\mu$ -oxido)-bridged  $\text{Mn}^{\text{III,IV}}_2$  core species exhibits a ca. 1110 G wide signal, distinguishable from the signal of a bis( $\mu$ -oxido)-bridged  $\text{Mn}^{\text{III,IV}}_2$  core that is typically 140 G wider.<sup>[32]</sup> The relative peak intensities of the  $\text{Mn}^{\text{III,IV}}_2$  spectrum detected here, however, differ from those reported for compounds where the two manganese centers are only bridged by a single oxido ligand. We attribute this to the distinction in magnetic coupling pattern based on the fact that the compound reported here has an additional bridging phenolato oxygen atom also contributing to the magnetic communication.

Coulometric measurements show that 40% of **1** is converted at this potential to the  $\text{Mn}^{\text{III,IV}}_2$  species. In dry solutions, the same experimental conditions result in a similar  $\text{Mn}^{\text{III,IV}}_2$  signal, but this is superimposed by a six-line signal, resulting in a 19-line spectrum as described in our previous study (see Supporting Information, Figure S2).<sup>[26]</sup> The development of a 6-line signal indicates the formation of monomeric Mn species as a result of further oxidation (vide infra). The presence of water therefore seems to stabilize the  $\text{Mn}^{\text{III,IV}}_2$  state to some degree, preventing further oxidation to monomeric species. At high  $\text{H}_2\text{O}$  concentration ( $> 5$  M), six-line EPR signal appear (not shown), suggesting that hydrolysis and redox-disproportionation reactions of **1** occur at high water concentrations.<sup>[33]</sup>

If the applied oxidising potential is increased by merely 60 mV to  $+0.70$  V, coulometry indicates that the oxidation process yields a total of 2 equiv. of electrons per 1 equiv. of **1**. An unknown fraction of **1** seems to be degraded under

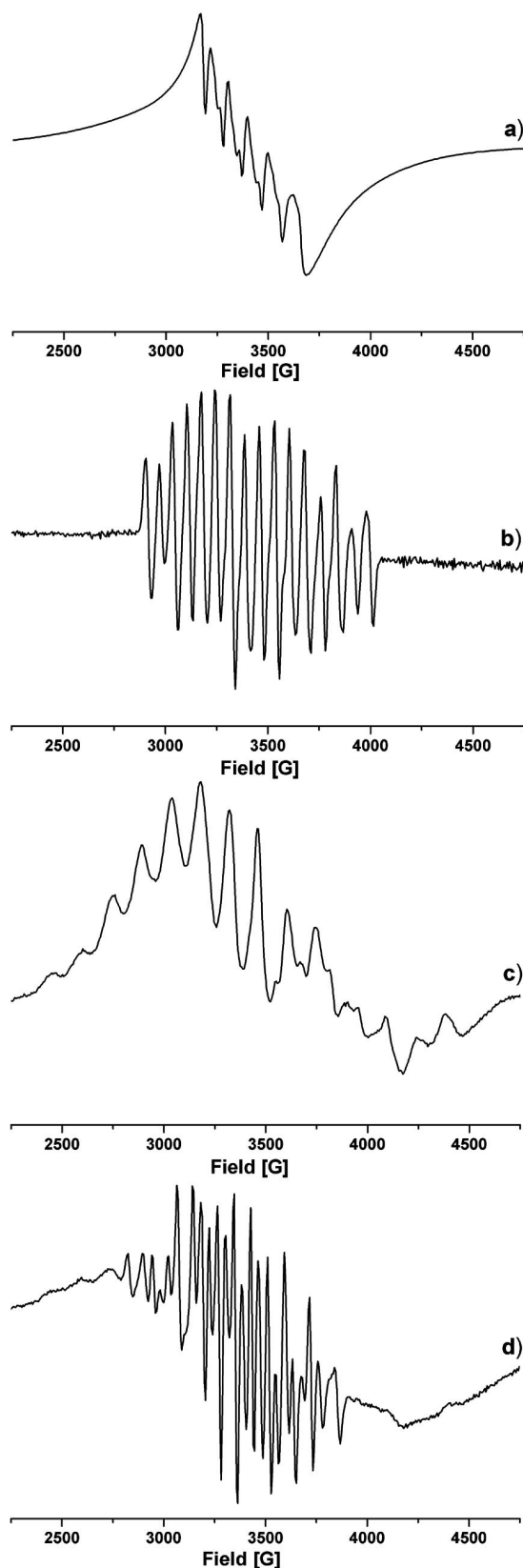


Figure 3. EPR spectra of solutions of **1** (1 mM) in MeCN/0.5 M H<sub>2</sub>O after bulk electrolysis at (a) +0.70 V (b) +0.64 V, (c) –0.51 V and (d) –1.01 V. EPR parameters for all measurements: temperature: 5 K, microwave frequency: 9.58 GHz; modulation amplitude: 10 G; microwave power: 2 mW.

these conditions to form manganese oxides, as the working electrode is coated by an insoluble brown precipitate during electrolysis. The EPR spectrum of the resulting solution after electrolysis is dominated by a six-line EPR signal, while the 16-line spectrum is not observable (Figure 3a), which suggests that oxidations at higher potentials result in the loss (probably due to oxidation) of the bridging phenolato ligand.

The EPR spectrum of samples after single-electron reduction at –0.51 V (coulombic yield 95%) in the presence of 0.5 M H<sub>2</sub>O shows a ca. 2000 G wide multiline signal centered at  $g \approx 2$  with ca. 150 G line spacings (Figure 3c). The presence of water does not significantly influence the appearance of this spectrum, which was also found in dry MeCN.<sup>[26]</sup> The wide spectral width and large line-splitting features have been observed for other Mn<sup>II,III</sup><sub>2</sub> species with similar core structures and were explained as a consequence of large anisotropies of the  $g$  factor, hyperfine coupling constant and line-width parameters.<sup>[34,35]</sup>

After further reduction of **1** at a potential of –1.01 V (coulombic yield 90% of one electron), an EPR spectrum is obtained which is a superposition of different spectral components (Figure 3d). A small fraction of the spectrum of residual Mn<sup>II,III</sup><sub>2</sub> complex is observed in the wings of the spectrum. Most interestingly, a well-resolved, unprecedented 25-line signal, centred at  $g \approx 2$  is found. The unusual 25-line signal is much narrower (ca. 1040 G) than Mn<sup>II,III</sup><sub>2</sub> and Mn<sup>III,IV</sup><sub>2</sub> multiline signals, particularly in hyperfine splittings, with average line spacings of ca. 42 G. Narrow line widths and nearly half of the intrinsic hyperfine coupling constants of Mn<sup>II</sup> (ca. 90 G) are usually interpreted as indications for an Mn complex with two equivalent spin centres.<sup>[36,37]</sup>

To the best of our knowledge, a similar signal has not been reported before for a dimeric manganese compound. Broad multi-line spectra with line spacing of ca. 40 G, similar at first sight to our 25-line spectrum, have been observed for many Mn<sup>II,II</sup><sub>2</sub> systems like arginase,<sup>[38]</sup> SoxB<sup>[39]</sup> or Mn<sup>II,II</sup><sub>2</sub> model compounds.<sup>[40]</sup> However, for these species line shapes are very temperature-dependent due to the involvement of higher spin states.<sup>[38]</sup> In addition, the spectral features of these known complexes are spread out over a region several thousand Gauss wide.

This is very different for the 25-line signal reported here, as this shows spectral features only in the  $g \approx 2$  region without contributions at other parts of the spectrum (see Supporting Information, Figure S3). The 25 lines retain their relative signal amplitude for a temperature range from 4 up to 50 K (not shown). No new signals were found for higher temperatures as observed for the other Mn<sup>II,II</sup><sub>2</sub> systems mentioned above. Importantly, the 25-line signal gradually decreased in signal amplitude in the entire spectral region with increasing temperature from 4 to 50 K, showing a non-linear Curie behavior (see Supporting Information, Figure S4).

As the species is formed under strongly reducing conditions and only little UV/Vis absorbance is observed after a double-electron reduction found by coulometry, we suggest



that this signal stems from an unusual  $\text{Mn}^{\text{II,II}}_2$  or  $\text{Mn}^{\text{II,III}}_2$  species that underwent a major structural change from **1**. No observable spectral changes in the presence of 0.5 M  $\text{H}_2\text{O}$  indicate that this  $\text{Mn}^{\text{II,II}}_2$  species does not strongly interact with water. We also note that these spectral features were not observed in our earlier study<sup>[26]</sup> under similar experimental conditions. This is attributed to the improved quality of **1** in this study.

The samples prepared by two-electron reduction at a potential of  $-1.01$  V were re-oxidized at a potential of  $+0.14$  V. The coulombic yield for this two-electron re-oxidation reaches 90%. The EPR spectrum of the resulting solution shows the narrow 25-line signal, retaining its signal amplitude whereas the rest of the EPR signal disappears (Figure 4). For a re-oxidation reaction carried out at an intermediate potential of  $-0.51$  V, a mixture of the 25-line and the  $\text{Mn}^{\text{II,III}}_2$  signal is found (see Supporting Information, Figure S5).

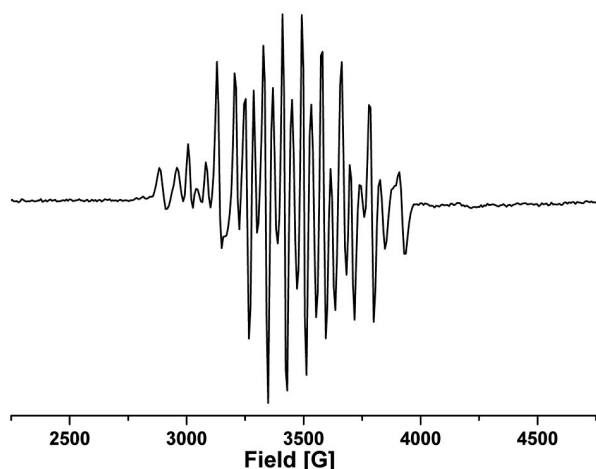


Figure 4. The 25-line EPR spectrum recorded for a solution of **1** (1 mM) in MeCN/0.5 M  $\text{H}_2\text{O}$  after bulk electrolysis at  $-1.01$  V and consecutive re-oxidation at  $+0.14$  V. Compare Figure 3 for EPR parameters.

These results from bulk-electrolysis experiments support the findings from the cyclic voltammetry and UV/Vis spectroelectrochemistry experiments described above. It is possible to reduce compound **1** in two steps from the EPR-silent  $\text{Mn}^{\text{III,III}}_2$  state via an  $\text{Mn}^{\text{II,III}}_2$  species to the  $\text{Mn}^{\text{II,II}}_2$  state. Most of the doubly reduced **1** (ca. 90%) can be successfully re-oxidized via the  $\text{Mn}^{\text{II,III}}_2$  intermediate to an EPR-silent  $\text{Mn}^{\text{III,III}}_2$  species, while a small fraction, transformed into the species responsible for the 25-line signal, cannot not be re-oxidized.

### Chemical Redox Reactions

The assignments of EPR signals to manganese redox states presented so far was examined further by experiments probing the reactivity of **1** towards chemical redox agents. Reactions of **1** with the very strong oxidizing agents  $\text{S}_2\text{O}_8^{2-}$ ,  $\text{Ce}^{4+}$  or  $\text{H}_2\text{O}_2$  seem to mainly result in the decomposition of the manganese dimer into monomeric compounds, as revealed by strong six-line EPR signals, similar to that shown

in Figure 3a. If the milder oxidation agents  $\text{Pb}^{4+}$  and  $\text{OCl}^-$  are used, the oxidation reaction leads to the formation of the  $\text{Mn}^{\text{III,IV}}_2$  oxidation state, indicated by 16-line spectra similar to Figure 3b. In the case of oxidation by  $\text{Pb}^{4+}$ , a radical signal, probably originating from the oxidation of one of the phenolato moieties of the ligand, is observed together with the 16-line signal from  $\text{Mn}^{\text{III,IV}}_2$  (Figure 5a).

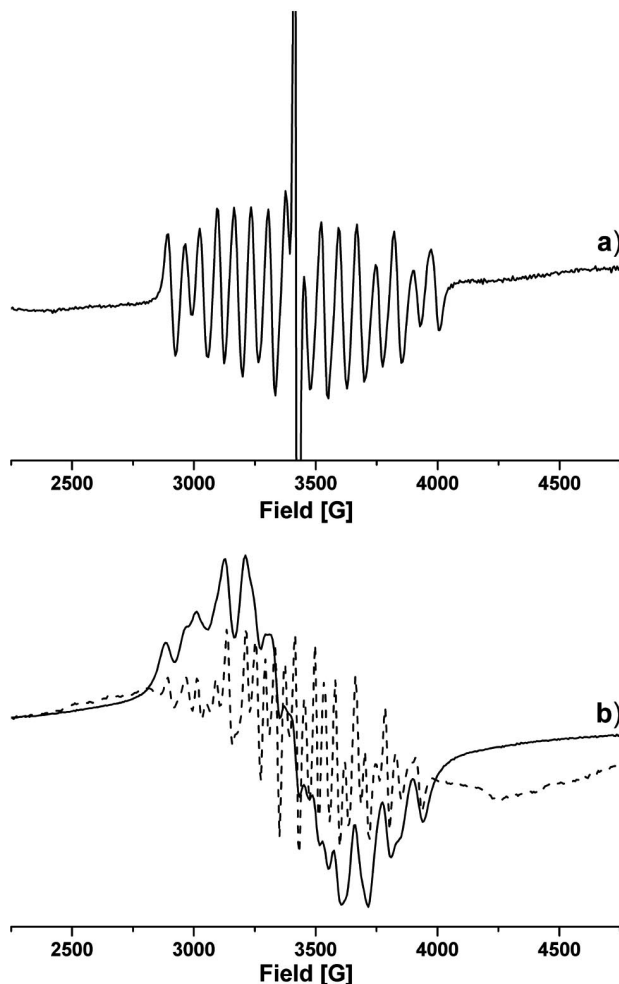


Figure 5. EPR spectra of solutions of **1** (1 mM) in MeCN/5 M  $\text{H}_2\text{O}$  after the addition of 10 equiv. of (a)  $\text{Pb}(\text{AcO})_4$  and (b)  $\text{NaBH}_4$  (—), respectively. In (b) the spectrum of a sample from bulk electrolysis at  $-1.01$  V (---, Figure 3d) is superimposed for comparison. Compare Figure 3 for EPR parameters.

Concerning reactions with chemical reductants, reactions with either  $\text{S}_2\text{O}_4^{2-}$  or  $\text{BH}_4^-$  resulted in complete decolourisation of the solution, indicating reduction to the  $\text{Mn}^{\text{II,II}}_2$  state. In the case of  $\text{S}_2\text{O}_4^{2-}$ , the EPR of the reaction mixture showed only a structureless, wide wave (not shown) with an overall line width and envelope line shape similar to the one underlying the multiline signal shown in Figure 3d, which could be assigned to a broadened  $\text{Mn}^{\text{II,III}}_2$  signal. When **1** is reduced by  $\text{BH}_4^-$ , the EPR spectrum showed an overall line width similar to the 25-line signal described above, even though with significantly broadened lines (Figure 5b). As the signal was much narrower than that for  $\text{Mn}^{\text{II,III}}_2$ , this oxidation state could be excluded.

It thus seems that all redox states of **1** accessible by electrochemical reactions can also be reached by reactions with chemical reagents. In the case of mild chemical oxidations, well-structured  $\text{Mn}^{\text{III,IV}}_2$  16-line signals were obtained. This agrees well with the observation that water presence enhances the formation of the  $\text{Mn}^{\text{III,IV}}_2$  state. Oxidations under harsh conditions, i.e. using strong oxidants or acidic conditions, cause the dimer to decompose into monomeric species of  $\text{Mn}^{\text{IV}}$  or  $\text{Mn}^{\text{II}}$ . Although the 6-line signal resembles a monomeric  $\text{Mn}^{\text{II}}$  6-line EPR signal very well, several monomeric  $\text{Mn}^{\text{IV}}$  species have been reported to exhibit similar 6-line EPR signals at  $g = 2$  with similar coupling constants (ca. 95 G) as found for  $\text{Mn}^{\text{II}}$ .<sup>[41,42]</sup> It is more likely that under our experimental conditions, where an excess of oxidant was used, the 6-line signal originates from  $\text{Mn}^{\text{IV}}$ . However, it can not be excluded that decomposition of the complex might lead to the formation of  $\text{Mn}^{\text{II}}$ .

When **1** is chemically reduced, the EPR spectra from both  $\text{Mn}^{\text{II,III}}_2$  and  $\text{Mn}^{\text{II,II}}_2$  states were formed but in both cases significantly broadened. This is due to the presence of product mixtures as a result of the influence of water, as the reactions were carried out by exposing **1** to a tenfold excess of the respective redox agent in the presence of 5 M water.

### Photooxidation Experiments

As the ultimate target reaction for the design of compounds like **1** is catalytic, light-driven water oxidation, it is of key importance to probe the possibility to oxidize such compounds photochemically in the presence of water. A widely used photosensitizer for oxidations is  $[\text{Ru}^{\text{II}}(\text{bipy})_3]^{2+}$ , which has been used as light-absorbing entity for photooxidations and as part of donor–acceptor diads together with manganese moieties by our group before.<sup>[7,33]</sup> The MLCT excited state of  $[\text{Ru}(\text{bipy})_3]^{2+}$ , generated by absorption of visible light photons, is a strong enough reduc-

ing agent to be able to reduce a range of different acceptor molecules. Reaction with an acceptor then generates the strongly oxidizing  $[\text{Ru}^{\text{III}}(\text{bipy})_3]^{3+}$  with an oxidation potential of +1.54 V.<sup>[43]</sup>

In the dark, we prepared reaction mixtures of **1**,  $[\text{Ru}^{\text{II}}(\text{bipy})_3]^{2+}$  and the irreversible electron acceptor 4-nitrobenzyl bromide (4-NBB)<sup>[44]</sup> in MeCN containing 0.5 M  $\text{H}_2\text{O}$ . Illumination by white light ( $\lambda > 400$  nm) results in one-electron oxidation of **1** within minutes from its original  $\text{Mn}^{\text{III,III}}_2$  state to an  $\text{Mn}^{\text{III,IV}}_2$  species, clearly detectable by EPR spectroscopy (Figure 6). If the solution is exposed to light for extended time, further oxidation to monomeric species is observed (Figure 6, dotted line). It is therefore possible to reach the same oxidation states of **1** by use of the photogenerated oxidant  $[\text{Ru}^{\text{III}}(\text{bipy})_3]^{3+}$  similar to electrochemical and chemical oxidations.

### Conclusions

The redox chemistry of **1** in MeCN/ $\text{H}_2\text{O}$  mixtures described in this study might be depicted as shown in Scheme 2. Starting from compound **1**, synthesized in its  $\text{Mn}^{\text{III,III}}_2$  state, two reversible reductions were detected to yield **1** in its  $\text{Mn}^{\text{II,III}}_2$  and  $\text{Mn}^{\text{II,II}}_2$  oxidation states. The effect of water on these reductions is small, and regular EPR signals, as expected for  $\text{Mn}^{\text{II,III}}_2$  and  $\text{Mn}^{\text{II,II}}_2$  species, are detected. We therefore conclude that the ligand framework surrounding the manganese atoms is not changed upon reduction and that the only processes occurring are metal-centered redox events.

However, a fraction of the doubly reduced **1**, the  $\text{Mn}^{\text{II,II}}_2$  species, undergoes ligand rearrangement into the species for which we observe the unprecedented 25-line EPR signal. The conversion seems irreversible, and the species cannot be re-oxidized. Considering the conditions at which this compound is formed, we suggest that the species is an  $\text{Mn}^{\text{II,II}}_2$  or  $\text{Mn}^{\text{II,III}}_2$  complex with a ligand environment greatly changed from that of **1**. Computational modelling of the 25-line signal together with magnetic measurements are currently being carried out to characterize this interesting new species in more detail.

The influence of water on the oxidation reactions of **1** is large. The presence of water seems to enhance the stability of  $\text{Mn}^{\text{III,IV}}_2$  species and leads to oxidations to occur at lower potentials. In the absence of water, a clean  $\text{Mn}^{\text{III,IV}}_2$  EPR signal of **1** could not be obtained, as oxidations are always accompanied by the decomposition of a fraction of the complex into monomeric  $\text{Mn}^{\text{II}}$  or  $\text{Mn}^{\text{IV}}$  species where coupling between the two manganese atoms is lost.<sup>[26]</sup> In contrast, we could prepare samples in the presence of water that show nothing but clean signals of mono( $\mu$ -oxido)-bridged  $\text{Mn}^{\text{III,IV}}_2$  species. It has been reported that an oxido-bridged  $\text{Mn}^{\text{III,IV}}_2$  species with a similar heptadentate ligand dimerizes to form  $(\text{Mn}^{\text{III,IV}}_2)_2$  tetramers containing four  $\mu$ -oxido bridges.<sup>[45]</sup> As such compounds are even spin systems, they are expected to be EPR-silent. The fact that we observe the characteristic

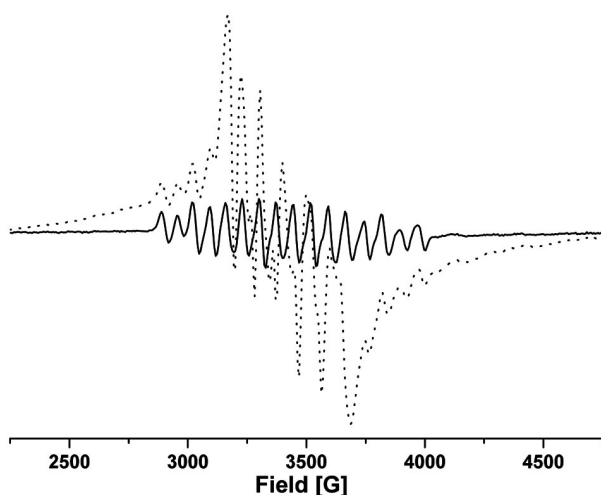
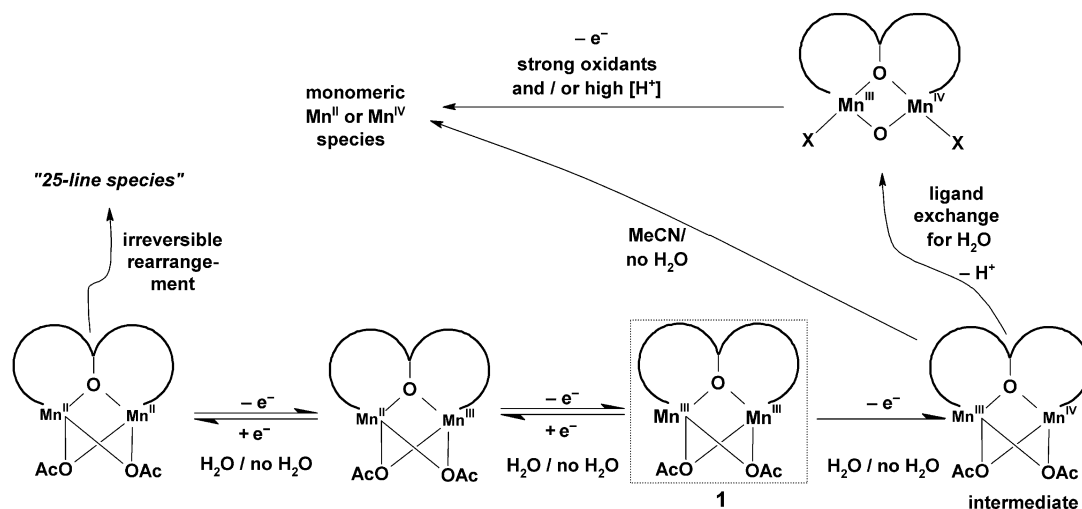


Figure 6. EPR spectra of a photooxidized solution of **1** (1 mM) in MeCN/0.5 M  $\text{H}_2\text{O}$ , in the presence of  $[\text{Ru}^{\text{II}}(\text{bipy})_3](\text{PF}_6)_2$  (4 mM) and 4-NBB (8 mM). Spectra after 5 min (—) and 45 min (···) illumination with white light ( $\lambda > 400$  nm). Compare Figure 3 for EPR parameters.



Scheme 2.

EPR signal for a dinuclear  $\text{Mn}^{\text{III,IV}}_2$  compound here indicates that the formation of a tetranuclear compound does not occur for **1**, most probably because of the steric hindrance caused by the *tert*-butyl substituents of the ligand.

We therefore propose here that the oxidation of **1** in a first step generates an intermediate  $\text{Mn}^{\text{III,IV}}_2$  species with an unchanged ligand set coordinated to the manganese centers. In the absence of water, this species is prone to attack by the MeCN solvent, and the ligand bridges between the manganese centers are lost, thereby deactivating the magnetic interaction between the Mn centers. Water, however, might replace one or both acetato ligands (Scheme 2) and form  $\mu$ -oxido bridge(s) between the two manganese centers that are known to stabilize dinuclear manganese complexes in higher oxidation states.<sup>[9,25]</sup> Only the use of very strong oxidants or acidic conditions causes the decomposition of **1** in the presence of water.

In conclusion, we find two major effects of even small concentrations of water on the redox chemistry of compound **1**:

- the overall potential span needed to reach the highest oxidation state of **1** ( $\text{Mn}^{\text{III,IV}}_2$ ) from its most reduced state ( $\text{Mn}^{\text{II,II}}_2$ ) becomes significantly smaller.
- higher oxidation states are stabilized, most likely by water coordination and the formation of  $\mu$ -oxido bridge(s) between the two manganese atoms.

To reach the goal of catalytic water oxidation with compounds like **1**, it is necessary to reach high manganese oxidation states. The mentioned effects seem to indicate that the substrate, water itself, might help us on the way to reach this goal.

## Experimental Section

**General:** All chemicals were of reagent grade and used as received. The ligand  $\text{H}_3\text{L}$  was prepared according to a published procedure.<sup>[26]</sup> The dimanganese(III) complex of the deprotonated form of  $\text{H}_3\text{L}$ ,  $[\text{Mn}_2\text{L}(\mu\text{-OAc})_2]^+$  was prepared similarly as reported before,<sup>[26]</sup> but isolated as the crystalline perchlorate salt  $[\text{Mn}_2\text{L}(\mu\text{-OAc})_2](\text{ClO}_4)_2$  (**1**· $\text{ClO}_4$ ) for this study, which significantly improved the purity of the product. IR spectra were recorded with a Perkin–Elmer Spectrum 100 FTIR spectrometer; a Finnigan LCQ Deca XP Max ESI-MS was used to obtain mass spectra.

**CAUTION!** Perchlorate salts of metal complexes are potentially explosive.

**$[\text{Mn}_2\text{L}(\mu\text{-OAc})_2]\text{ClO}_4$  (**1**· $\text{ClO}_4$ ):**  $\text{Mn}(\text{OAc})_3 \cdot 2\text{H}_2\text{O}$  (143.8 mg, 0.54 mmol) was added in one portion to an ethanol solution (3 mL) of  $\text{H}_3\text{L}$  (154.6 mg, 0.20 mmol). The dark red-brown solution was heated to 50 °C under argon for 20 min. A solution of  $\text{NaClO}_4 \cdot \text{H}_2\text{O}$  (93.4 mg, 0.66 mmol) in ethanol (1 mL) was then added, the reaction mixture was slowly cooled to room temperature and afterwards kept at –18 °C for 48 h. A dark red-brown solid precipitated which was filtered off and washed with cold ethanol and diethyl ether. Re-crystallisation from ethanol yielded **1** as dark red-brown microcrystalline powder (180 mg, 80%). IR (ATR):  $\tilde{\nu}$  = 2950, 2905 (w, C–H), 1573 (vs, –COO), 1441 (m, arom. rings), 1089 (vs,  $\text{ClO}_4^-$ ), 758 (m)  $\text{cm}^{-1}$ . ESI-MS (MeCN):  $m/z$  = 1009.5  $[\text{M}]^+$  (showing the isotope pattern calculated for  $\text{C}_{55}\text{H}_{71}\text{Mn}_2\text{N}_4\text{O}_7$ ).  $\text{C}_{55}\text{H}_{71}\text{ClMn}_2\text{N}_4\text{O}_{11}$  (1109.5): calcd. C 59.54, H 6.45, N 5.05; found C 59.38, H 6.53, N 4.91.

**Electrochemistry:** Cyclic voltammetry and controlled potential electrolysis were carried out by using an Autolab potentiostat with a GPES electrochemical interface (Eco Chemie). Sample solutions (4 mL) were prepared from dry acetonitrile and de-ionized water (MilliQ) containing 0.1 M tetrabutylammonium (TBA) perchlorate (Fluka, electrochemical grade) as supporting electrolyte. For cyclic voltammetry, the working electrode was a glassy carbon disc (diameter 3 mm). All cyclic voltammograms shown were recorded at a scan rate of 0.1  $\text{V s}^{-1}$ . A glassy carbon rod served as counter electrode, and the reference electrode was an  $\text{Ag}/\text{Ag}^+$  electrode (a silver wire immersed into 10 mM  $\text{AgNO}_3$  in MeCN) with a potential of –0.07 V vs. the ferrocene/ferrocenium ( $\text{Fc}/\text{Fc}^+$ ) couple in dry MeCN. Counter and reference electrode were in compartments separated from the bulk solution by fritted disks and were the same for all analytical, bulk and spectroelectrochemical experiments. All potentials reported here are given relative to the  $\text{Fc}/\text{Fc}^+$  couple in MeCN solutions containing the respective concentrations of water, as the potential of the  $\text{Fc}/\text{Fc}^+$  couple vs.  $\text{Ag}/\text{Ag}^+$  was found to change for MeCN containing increasing  $\text{H}_2\text{O}$  concentrations (a known phenomenon for aqueous/organic mixtures<sup>[46,47]</sup>). Before all measurements, oxygen was removed by bubbling solvent-saturated



argon through the stirred solutions. Samples were kept under argon during measurements. To obtain EPR spectra of **1** in different oxidation states, solutions prepared in the same way as described above for analytical electrochemistry were subjected to bulk electrolysis at controlled potentials. A cylindrical platinum grid (ca. 4 cm<sup>2</sup>) was used as working electrode for bulk electrolysis. Electrolyses were monitored by amperometry and coulometry and took 3–5 min to completion. After electrolysis, samples of 200 µL were taken from the solution with an air-tight, argon-filled syringe, transferred to argon-flushed EPR tubes, frozen and stored in liquid nitrogen. For the preparation of samples showing only the unusual 25-line EPR signal (Figure 4), solutions of **1** (1 mM) in MeCN containing 0.5 M H<sub>2</sub>O and 0.1 M TBA·ClO<sub>4</sub> were prepared. These were subjected to bulk electrolysis applying a potential of –1.01 V for 3 min. The potential was then switched to +0.14 V to re-oxidise the sample at this potential within another 3 min.

**UV/Vis Spectroelectrochemistry:** Solutions of **1** were prepared in the same way as described above for analytical electrochemistry and filled into an argon-purged OTTLE quartz cell (path length 1 mm). A platinum grid (10 mm × 30 mm, 400 mesh) was used as working electrode. Electrolyses in the OTTLE cell took 10–15 min until completion during which time UV/Vis spectra were recorded with a Hewlett–Packard 8453 diode-array spectrometer.

**EPR Spectroscopy:** EPR spectra were recorded with a Bruker eleXsys E500 spectrometer equipped with an ER 4116DM dual-mode resonator. Samples were measured at 5 K using an Oxford 900 liquid helium cryostat and an ITC 503 temperature controller. Data analysis was performed with the Bruker Xepr 2.4b software package.

**Chemical Redox Reactions:** For chemical redox reactions, argon-purged solutions of **1** in MeCN and the redox agent in H<sub>2</sub>O were mixed at room temperature in argon-flushed EPR tubes to reach the following final concentrations (total volume 200 µL): **1**, 1 mM; redox agent, 10 mM; H<sub>2</sub>O, 5 M. After a reaction time of 5 min, samples were frozen and stored in liquid nitrogen.

**Photooxidation Experiments:** A solution of **1** (1 mM), [Ru(bipy)<sub>3</sub>](PF<sub>6</sub>)<sub>2</sub> (4 mM) and 4-nitrobenzyl bromide (8 mM) in MeCN/0.5 M H<sub>2</sub>O was prepared in the dark. 200 µL samples were filled into EPR tubes and air was removed by purging solution and EPR tube with argon. The samples were illuminated at 20 °C with visible light from a slide projector (Zeiss Icon Voigtländer S 250 equipped with a 250-W Osram Xenophot HLX lamp). A cut-off filter (Schott GG 400) was placed between projector and sample to ensure that only visible light (λ > 400 nm) reached the samples. After illumination, samples were immediately frozen in liquid nitrogen and transferred to the EPR spectrometer for measurements.

**Supporting Information** (see footnote on the first page of this article): ESI-MS spectra, additional EPR spectra, temperature dependence of the 25-line EPR signal.

## Acknowledgments

This work was supported by grants from the Swedish Energy Agency, The Knut and Alice Wallenberg Foundation, The Swedish Research Council, NEST-STRP SOLAR-H (EU contract no. 516510) and Stiftelsen Bengt Lundqvists minne (P.H.). The authors also would like to thank Dr. Reiner Lomoth from Uppsala University for valuable discussions and Dr. John Kumar from Uppsala University for ESI-MS measurements.

[1] C. Goussias, A. Boussac, A. W. Rutherford, *Philos. Trans. R. Soc. London, Ser. B* **2002**, 357, 1369–1381.

- [2] M. Haumann, C. Muller, P. Liebisch, L. Iuzzolino, J. Dittmer, M. Grabolle, T. Neisius, W. Meyer-Klaucke, H. Dau, *Biochemistry* **2005**, 44, 1894–1908.
- [3] M. P. Klein, K. Sauer, V. K. Yachandra, *Photosynth. Res.* **1993**, 38, 265–277.
- [4] J. P. McEvoy, J. A. Gascon, V. S. Batista, G. W. Brudvig, *Photochem. Photobiol. Sci.* **2005**, 4, 940–949.
- [5] J. Yano, J. Kern, K. Sauer, M. J. Latimer, Y. Pushkar, J. Biesiadka, B. Loll, W. Saenger, J. Messinger, A. Zouni, V. K. Yachandra, *Science* **2006**, 314, 821–825.
- [6] M. Yagi, M. Kaneko, *Chem. Rev.* **2001**, 101, 21–35.
- [7] L. C. Sun, L. Hammarström, B. Åkermark, S. Styring, *Chem. Soc. Rev.* **2001**, 30, 36–49.
- [8] W. Ruttiger, G. C. Dismukes, *Chem. Rev.* **1997**, 97, 1–24.
- [9] S. Mukhopadhyay, S. K. Mandal, S. Bhaduri, W. H. Armstrong, *Chem. Rev.* **2004**, 104, 3981–4026.
- [10] E. Amouyal, *Sol. Energy Mater. Sol. Cells* **1995**, 38, 249–276.
- [11] J. Limburg, J. S. Vrettos, H. Y. Chen, J. C. de Paula, R. H. Crabtree, G. W. Brudvig, *J. Am. Chem. Soc.* **2001**, 123, 423–430.
- [12] C. Tommos, G. T. Babcock, *Biochim. Biophys. Acta* **2000**, 1458, 199–219.
- [13] I. Vass, S. Styring, *Biochemistry* **1991**, 30, 830–839.
- [14] P. Geijer, F. Morvaridi, S. Styring, *Biochemistry* **2001**, 40, 10881–10891.
- [15] H. Dau, M. Haumann, *Science* **2006**, 312, 1470–1472.
- [16] H. Y. Chen, R. Tagore, S. Das, C. Incarvito, J. W. Faller, R. H. Crabtree, G. W. Brudvig, *Inorg. Chem.* **2005**, 44, 7661–7670.
- [17] N. Kitajima, U. P. Singh, H. Amagai, M. Osawa, Y. Morooka, *J. Am. Chem. Soc.* **1991**, 113, 7757–7758.
- [18] C. Mukherjee, T. Weyhermüller, K. Wieghardt, P. Chaudhuri, *Dalton Trans.* **2006**, 2169–2171.
- [19] A. K. Poulsen, A. Rompel, C. J. McKenzie, *Angew. Chem. Int. Ed.* **2005**, 44, 6916–6920.
- [20] N. Wiberg, A. Holleman, E. Wiberg, *Inorganic Chemistry*, Academic Press, San Diego, London, **2001**.
- [21] B. Loll, J. Kern, W. Saenger, A. Zouni, J. Biesiadka, *Nature* **2005**, 438, 1040–1044.
- [22] K. N. Ferreira, T. M. Iverson, K. Maghlaoui, J. Barber, S. Iwata, *Science* **2004**, 303, 1831–1838.
- [23] P. Huang, P. Kurz, S. Styring, *Appl. Magn. Reson.* **2007**, 31, 301–320.
- [24] M. F. Anderlund, J. Höglblom, W. Shi, P. Huang, L. Eriksson, H. Weihe, S. Styring, B. Åkermark, R. Lomoth, A. Magnuson, *Eur. J. Inorg. Chem.* **2006**, 5033–5047.
- [25] G. Eilers, C. Zettersten, L. Nyholm, L. Hammarström, R. Lomoth, *Dalton Trans.* **2005**, 1033–1041.
- [26] R. Lomoth, P. Huang, J. T. Zheng, L. C. Sun, L. Hammarström, B. Åkermark, S. Styring, *Eur. J. Inorg. Chem.* **2002**, 2965–2974.
- [27] Y. Nishida, M. Nasu, *Inorg. Chim. Acta* **1991**, 190, 1–3.
- [28] L. Dubois, F. Caspar, L. Jacquamet, P. E. Petit, M. F. Charlot, C. Baffert, M. N. Collomb, A. Deronzier, J. M. Latour, *Inorg. Chem.* **2003**, 42, 4817–4827.
- [29] In earlier experiments, residual EPR signals for **1**, assigned to originate from Mn<sup>II,III</sup><sub>2</sub> and Mn<sup>III,IV</sup><sub>2</sub> species, were detected in dry MeCN, which indicated that the prior isolation method as a PF<sub>6</sub><sup>–</sup> salt was less advantageous, as it resulted in the coprecipitation of impurities.
- [30] O. Horner, E. Anxolabehere-Mallart, M. F. Charlot, L. Tchertanov, J. Guilhem, T. A. Mattioli, A. Boussac, J. J. Girerd, *Inorg. Chem.* **1999**, 38, 1222–1232.
- [31] C. Hureau, G. Blondin, M. F. Charlot, C. Philouze, M. Nierlich, M. Cesario, E. Anxolabehere-Mallart, *Inorg. Chem.* **2005**, 44, 3669–3683.
- [32] C. Hureau, L. Sabater, E. Anxolabehere-Mallart, M. Nierlich, M. F. Charlot, F. Gonnet, E. Riviere, G. Blondin, *Chem. Eur. J.* **2004**, 10, 1998–2010.
- [33] P. Huang, J. Höglblom, M. F. Anderlund, L. C. Sun, A. Magnuson, S. Styring, *J. Inorg. Biochem.* **2004**, 98, 733–745.



- [34] H. Diril, H. R. Chang, M. J. Nilges, X. H. Zhang, J. A. Potenza, H. J. Schugar, S. S. Isied, D. N. Hendrickson, *J. Am. Chem. Soc.* **1989**, *111*, 5102–5114.
- [35] P. Huang, N. Shaikh, M. F. Anderlund, S. Styring, L. Hammarström, *J. Inorg. Biochem.* **2006**, *100*, 1139–1146.
- [36] A. Bencini, D. Gatteschi, *EPR of Exchange Coupled Systems*, Springer, Berlin, Heidelberg, New York, **1990**.
- [37] J. Owen, E. A. Harris, in *Electron Paramagnetic Resonance* (Ed.: E. Geschwind), Plenum Press, New York, **1972**.
- [38] S. V. Khangulov, P. J. Pessiki, V. V. Barynin, D. E. Ash, G. C. Dismukes, *Biochemistry* **1995**, *34*, 2015–2025.
- [39] B. Epel, K. O. Schäfer, A. Quentmeier, C. Friedrich, W. Lubitz, *J. Biol. Inorg. Chem.* **2005**, *10*, 636–642.
- [40] D. P. Kessissoglou, W. M. Butler, V. L. Pecoraro, *Inorg. Chem.* **1987**, *26*, 495–503.
- [41] C. R. Byfleet, W. C. Lin, C. A. McDowell, *Mol. Phys.* **1970**, *18*, 363–370.
- [42] M. M. Morrison, D. T. Sawyer, *Inorg. Chem.* **1978**, *17*, 338–339.
- [43] G. J. Kavarnos, N. J. Turro, *Chem. Rev.* **1986**, *86*, 401–449.
- [44] S. N. J. Moreno, J. Schreiber, R. P. Mason, *J. Biol. Chem.* **1986**, *261*, 7811–7815.
- [45] M. K. Chan, W. H. Armstrong, *J. Am. Chem. Soc.* **1990**, *112*, 4985–4986.
- [46] M. Hecht, W. R. Fawcett, *J. Phys. Chem.* **1996**, *100*, 14240–14247.
- [47] P. A. Lay, N. S. McAlpine, J. T. Hupp, M. J. Weaver, A. M. Sargeson, *Inorg. Chem.* **1990**, *29*, 4322–4328.

Received: August 28, 2007

Published Online: January 3, 2008